EPJ Web of Conferences **56**, 01010 (2013)
DOI: 10.1051/epjconf/20135601010

Experimental Study of Contaminant Release from Reducing Grout

R.T. Pabalan[1], G.W. Alexander[2], D.J. Waiting[1], and C.S. Barr[2]

[1]Center for Nuclear Waste Regulatory Analyses, San Antonio, Texas, U.S.A.
[2]U.S. Nuclear Regulatory Commission, Washington, D.C., U.S.A.

Abstract. A column experiment was conducted to study the release behavior of technetium, uranium, and selenium initially sequestered in reducing grout similar in composition to Savannah River Site (SRS) saltstone, a cementitious waste form made by mixing salt solution from SRS liquid waste storage tanks with a dry mix containing blast furnace slag, fly ash, and Portland cement. The data suggest that uranium was retained in the grout possibly as a $CaUO_4$ phase, whereas most of the selenium was released. Technetium release initially was relatively constant, and then increased significantly after 26 pore volumes. The increase in technetium release was slightly delayed relative to the observed Eh increase. The system Eh–pH started under conditions in which technetium solubility is low, constrained by Tc_3O_4 solubility, but eventually transitioned into the stability field of the pertechnetate ion. The delay in technetium release relative to the Eh increase was possibly due to slow oxidation of technetium at depth within the grout particles, which in turn was likely controlled by O_2 diffusion into the particles. In contrast to technetium and uranium, selenium release was not solubility limited and selenium likely was present in the pore solution initially as a HSe^- species.

1 Introduction

The ability of cement-based materials (e.g., grout) to serve as barriers to groundwater influx and to radionuclide release and transport is an important factor in U.S. Department of Energy (DOE) performance assessments related to tank closure and low-activity waste disposal in near-surface disposal facilities. A key factor determining the release and transport of redox sensitive radionuclides (e.g., Tc-99, Np-237, U-233, and Se-79) is the redox potential and reduction capacity of the cement-based material. Studies have shown that grouted systems containing blast furnace slag are effective in mitigating the release of Tc-99 [1–2]. Hydration of the blast furnace slag in the grout mixture releases sulfide species into the pore fluid, predominantly as S^{2-}, which can impose a strongly reducing redox potential (Eh) on the system [3] and can react with technetium to form relatively insoluble Tc_3S_{10} [4] or Tc_2S_7 [5]. In cementitious systems, U(IV) is less soluble than U(VI) [6] and Se(IV) (as the selenite ion, SeO_3^{2-}) is less mobile than Se(VI) (as the selenate ion, SeO_4^{2-}) [7].

However, the long-term persistence of the reducing capabilities of slag-bearing grout and its ability to mitigate the release of redox-sensitive radioelements is uncertain. Oxygen (O_2) in the gas

phase or dissolved in infiltrating water could react with and decrease the reductive capacity of slag. Calculations have been performed on O_2 oxidation of reducing grout to evaluate the longevity of low Eh conditions of grouted systems for radioactive waste disposal [8–9], but few experimental data are available for comparison with the calculated results and for correlating the changes in grout system chemistry with radionuclide release.

In this study, a column experiment was conducted to determine the release behavior of technetium, uranium, and selenium initially sequestered in reducing grout as O_2-bearing water interacts with the grout and changes the system chemistry. The study reacted grout that has a composition similar to Savannah River Site (SRS) saltstone with an SRS groundwater simulant. Technetium, uranium, and selenium release was studied because these radioelements are important risk drivers in some performance assessment calculations [10–11]. Also, limited published data are available on uranium and selenium release from slag-bearing grout.

2 Materials and Methods

Simulated saltstone was prepared from dry solids components (Type I//II Portland cement, Class F fly ash, and Grade 120 blast furnace slag) and a non-radioactive simulant of SRS tank waste solution using the recipe and formulation taken from [10] and shown in Table 1. Reference [10] provided recipes and formulations for the three SRS waste stream types: (i) Deliquifaction, Dissolution, and Adjustment (DDA); (ii) Salt Waste Processing Facility, and (iii) Modular Caustic Side Solvent Extraction Unit. The weight percentage of cement, fly ash, and slag in the dry mix is 10, 45, and 45, respectively, and the saltstone nominal blend composition is 5 wt% cement, 25 wt% fly ash, 25 wt% blast furnace slag, and 45 wt% salt solution [11]. The DDA waste simulant formulation was used in this study because DOE considered them to be representative of most of the waste streams going to the SRS Saltstone Facility [11].

Two batches of simulated saltstone were prepared: one with no contaminant and a second one containing Tc-99, U-238, and selenium. In preparing the second batch, the following were added to

Table 1. Recipe and formulation for Deliquifaction, Dissolution, and Adjustment (DDA) simulant solution, premix, and simulated saltstone [10]

DDA Simulant Components	**Molarity**	**Molecular Weight (g/mol)**	**Amount per Liter Solution (g)**
NaOH (50 wt% solution)	0.769	40.00	61.52
$NaNO_3$	2.202	84.99	187.15
$NaNO_2$	0.110	68.99	7.56
Na_2CO_3	0.145	105.99	15.36
Na_2SO_4	0.044	142.04	6.31
$Al(NO_3)_3{\cdot}9H_2O$	0.071	375.13	26.63
$Na_3PO_4{\cdot}12H_2O$	0.008	380.12	3.22
Premix Components		**Amount (g)**	
Blast Furnace Slag†		812	
Fly Ash‡		812	
Portland Cementə		180	
Total		1,804	
Simulated Saltstone Components		**Amount (g)**	
Premix		1,804	
DDA Simulant Solution*		1,396	
*Two liters of simulant solution were prepared † ASTM C989 Grade 120; Holcim, Inc., Supplier ‡Class F; Boral Material Technologies, Supplier 'Type I/II; Alamo Concrete Products, Supplier			

the DDA simulant solution prior to mixing with the dry solids components: (i) a Tc-99 spike comprised of 101.5 μCi of Tc-99 (as ammonium pertechnetate) in 5 g of water, (ii) 60 mL of a 0.05-M U-238 solution, and (iii) 1.40 g of reagent grade K_2SeO_4. The contaminant-bearing simulated saltstone was used in the column leaching experiment, whereas the uncontaminated simulated saltstone was used for grout material characterization.

To make each batch of simulated saltstone, the solid components were blended with the DDA simulant in a Hobart mixer. The grout was poured into a cylindrical plastic mold (10.3-cm inner diameter by 20.3-cm length) and allowed to cure for 28 days in the capped plastic mold. After curing, the contaminant-bearing simulated saltstone cylinder initially was broken up into 2.5- to 5-cm pieces using a sledge hammer, then crushed with the aid of a Sepor (Sepor, Inc., Wilmington, California) mini-jaw crusher with a tungsten carbide jaw and cheek plates. The crushed material was dry sieved to the size range <0.50 and >0.105 mm and stored in an N_2(g) atmosphere to minimize oxidation of the slag.

No attempt was made to keep an O_2-free environment during preparation of the grout material for the column experiment. The crushed and sieved grout material likely would have undergone some degree of oxidation before the experiment began, which could affect the contaminant release.

Simulated SRS groundwater was prepared by diluting by a factor of 100× a stock solution made from reagent grade NaCl, KCl, $CaSO_4 \cdot 2H_2O$, $MgCl_2 \cdot 6H_2O$, and $CaCl_2 \cdot 2H_2O$ (4.22, 1.25, 1.31, 1.69, and 4.93, mmol/L, respectively). Because the simulated SRS groundwater is dilute (ionic strength ~ 0.4 mmol/L), which is typical of SRS aquifer waters [12], the chemistry of the column effluent solution is expected to be dominated by its interaction with the grout material and contaminant release from the grout would not be expected to change significantly if other SRS groundwater compositions were used. The solution was not deaerated and was assumed to be O_2-saturated.

The column experiment used an acrylic flow cell (Soil Measurement Systems, Tucson, Arizona) with a 3.8-cm internal diameter, a 23-cm length, and endplates with a porous nylon membrane. The calculated internal volume of the flow cell is 260 mL. The cell was dry loaded with the crushed and sieved contaminant-bearing grout material and was tapped on the side intermittently during loading to increase the density of the packed material. The total grout mass loaded into the cell was 242 g.

The simulated SRS groundwater was pumped from a 1-L solution reservoir upwards through the flow cell using an Agilent 1100 high-performance liquid chromatography (HPLC) pump. The flow rate was set at 0.066 mL/min [95 mL/day]. Downstream of the grout column, two acrylic, microflow cells (Lazar Research Laboratories, Los Angeles, California) were connected in series—one with a microflow-through pH electrode and the other with a microflow-through redox electrode. Both pH and redox electrodes have an epoxy electrode body, an Ag/AgCl (with 4-molar KCl solution) internal reference electrode, and internal volumes less than 50 μL. Downstream of the microflow cells, a 1-L Tedlar® bag (SKC, Inc., Eighty Four, Pennsylvania) collected the effluent solutions. The Tedlar bag was replaced as it approached capacity.

Aqueous samples for chemical analysis were taken periodically by disconnecting the Tedlar bag and allowing the solution to collect into a preweighed 50-mL polypropylene bottle. To collect the 50-mL samples in a reasonable amount of time, the pump flow rate was increased to 0.5 mL/min during the sampling period. Two 1-mL aliquots from each of the aqueous samples were taken to measure Tc-99 activity, and the remainder was preserved for later analysis of cation and anion concentration. The sample pH also was measured using an Orion ROSS combination pH electrode for comparison with the pH determined using the microflow-through pH electrode.

The Tc-99 activity of the aqueous samples was measured using a liquid scintillation counter. Sodium, potassium, calcium, silicon, and aluminum were measured using inductively coupled plasma–optical emission spectrometry (ICP–OES), whereas uranium, selenium, and iron were measured using inductively coupled plasma–mass spectrometry (ICP–MS). Nitrate, nitrite, and sulfate concentrations were measured using ion chromatography.

The composition of the nonradioactive simulated saltstone was determined using x-ray fluorescence (XRF) analysis and x-ray diffraction (XRD) analysis. The surface area of the material

used in the column experiment was determined using a multipoint N_2-BET isotherm surface area analyzer and its bulk density was measured using a pycnometer.

3 Results

The interior and sides of the simulated saltstone cylinders that were cured in the plastic mold are greenish gray in color, with a white layer formed on the top surface. The white material is calcium carbonate based on a brisk effervescent reaction with dilute hydrochloric acid, which is characteristic of calcium carbonate, and confirmed by XRD data. Calcium carbonate formed due to the reaction of the alkaline, calcium-rich cement pore fluid with atmospheric CO_2(g).

The XRD patterns of the greenish gray and white simulated saltstone material indicated the presence of quartz; the calcium carbonate minerals aragonite, calcite, and vaterite; and the aluminosilicate minerals sillimanite and mullite. The latter two minerals are high-temperature mineral phases that likely were present in the blast furnace slag or fly ash component of the grout mixture. The calcium carbonate diffraction peaks of the XRD pattern of the white simulated saltstone material are ~2× higher compared to the greenish gray material.

The chemical compositions of the contaminant-free simulated saltstone, blast furnace slag, and fly ash determined using XRF analysis are reported in [13]. The measured specific surface area, bulk density, and total mass of grout material loaded into the flow cell are 32.9 m^2/g, 1.92 g/cm^3, and 242 g, respectively. The calculated volume and initial porosity of the grout material in the column are 126 cm^3 and 52 percent.

During the initial stages of the experiment, gas bubbles were observed to form in the columns as the simulated SRS groundwater reacted with the reducing grout, but their formation abated after several pore volumes (PVs) of simulated groundwater had reacted with the reducing grout. The gases are most likely H_2(g) and H_2S(g), based on the reducing character of the grout and the presence of sulfide in the blast furnace slag. The presence of H_2S(g) also was indicated by a "rotten egg" smell of some of the effluent solutions. Reduced sulfur species, mainly as thiosulfate, also was observed from the ion chromatography analyses.

The results are presented in terms of number of PVs, which was calculated from the equation

$$n_{pv} = \frac{f \cdot t}{V_c \cdot \phi} \tag{1}$$

where n_{pv} , f, t, V_c, and ϕ are the number of PVs, flow rate (mL/min), cumulative time (min), flow cell internal volume (mL), and effective porosity, respectively. As indicated previously, the flow cell internal volume is 260 mL and the initial porosity of the grout material in the flow cell is 52 percent. Thus, 1 PV (= $V_c \times \phi$) is equal to 135 mL.

The use of Eq. (1) assumes the effective porosity is invariant with time. In calculating the number of PVs of solution that flowed through the column, detailed accounting was made of the duration and flow rate when the HPLC pump was on. This procedure is important because the solution flow frequently had to be interrupted (e.g., to take samples, replace Tedlar bags, or fix leaks in the pH or Eh microflow cells) and the flow rate during sampling was higher (0.5 mL/min) than the normal flow rate of 0.066 mL/min.

Data on contaminant (e.g., technetium, nitrate, nitrite, selenium) release also are presented in terms of cumulative amount or fraction leached from the simulated saltstone. These quantities are calculated using the following equations

$$n_{cum,N}(t) = \sum_{i=1}^{t} (\Delta n_{pv,i} \cdot V_c \cdot \phi \cdot M_{s,N,i} / 1000) \tag{2}$$

$$F_{cum,N}(t) = \frac{n_{cum,N}(t)}{n_{t,N}} \tag{3}$$

where

$n_{cum,N}(t)$	=	cumulative number of moles of contaminant (N) leached from the grout at time t
$M_{s,N,i}$	=	measured contaminant molarity (mol/L) in the aqueous sample taken at time t_i
$n_{t,N}$	=	total moles of contaminant initially in the grout column
$F_{cum,N}(t)$	=	cumulative mole fraction of contaminant leached from the grout column at time t
$\Delta n_{pv,i}$	=	PV of solution that exited the column between time t_i and t_{i-1}

The initial amounts ($n_{t,N}$) of technetium, uranium, and selenium in the flow cell grout are equal to 4.49×10^{-6}, 6.56×10^{-4}, and 2.22×10^{-4} moles, respectively, based on the Tc-99 activity in the technetium spike, the uranium and selenium mass added to the grout mix, and the mass of grout material in the column. The initial amount of nitrate and nitrite in the cell is 0.194 and 9.70×10^{-3} moles, respectively, based on the nitrate and nitrite concentration in the DDA simulant solution and the amount of grout material in the column.

Figure 1 shows the measured effluent solution Eh as a function of PV. The Eh initially was high (+414 mV) due to dissolved O_2 in the groundwater simulant, but the system quickly became very reducing as the solution reacted with the reducing grout. After attaining a low Eh of −453 mV at 6 PVs, the system Eh relatively quickly increased to higher values (0 mV at 15 PVs and +180 mV at 22 PVs). Further Eh increases were more gradual and an Eh of +272 mV was measured at 132 PVs.

Figure 1 also shows the effluent solution pH measured using the Lazar microflow-through pH electrode and the Orion ROSS combination pH electrode. The pH initially was 11.4, then increased to 12.9 after two PVs as the solution reacted with the alkaline grout. Subsequently, the pH fell continuously for about 16 PVs to a value of 11.5. After 18 PVs, the pH remained relatively stable, varying between 11.3 and 11.5 up to 83 PVs, with an average value of 11.4 ± 0.1. The pH values measured with the Lazar and Orion pH electrodes were in good agreement through the first 83 PVs, after which the two measurements started to diverge, with the former averaging 11.5 and the latter averaging 11.3 at PVs >83. The divergence is likely due to a drift in the Lazar pH electrode, which was not recalibrated after the experiment started.

The measured aqueous concentrations in the effluent solution are plotted in Figure 2. Sodium, potassium, selenium, and sulfate concentrations decreased significantly through the first 20 PVs,

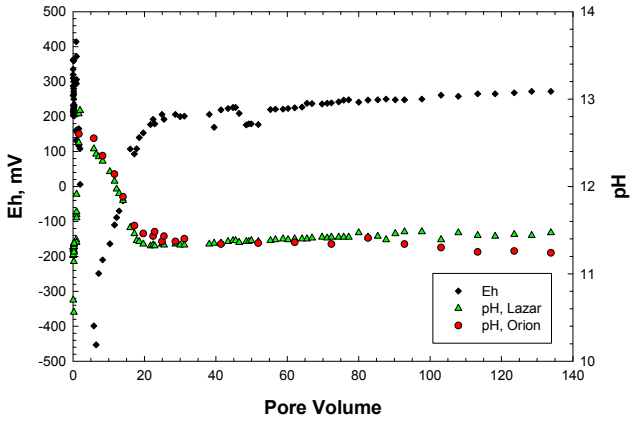

Fig. 1. Measured effluent solution pH and Eh as a function of number of PVs

then subsequently decreased more slowly. Calcium concentration decreased during the first 6 PVs, increased significantly through the next 20 PVs, then was relatively constant afterwards. Silicon concentration initially increased, then decreased significantly up to 20 PVs, and then showed a slightly increasing trend afterwards. Aluminum concentration showed a similar initial increase, followed by a significant decrease up to 20 PVs, then a gradual decrease at higher PVs. Iron, nitrate, and nitrite concentrations quickly decreased below the reporting limit of the analytical method.

Figure 3 plots the cumulative fractions of technetium, selenium, nitrate, and nitrite leached from the grout column as a function of PV. Uranium values are not plotted, because the measured uranium concentrations were mostly below the ICP–MS detection limit (0.002 ppm), indicating uranium was retained in the simulated saltstone grout.

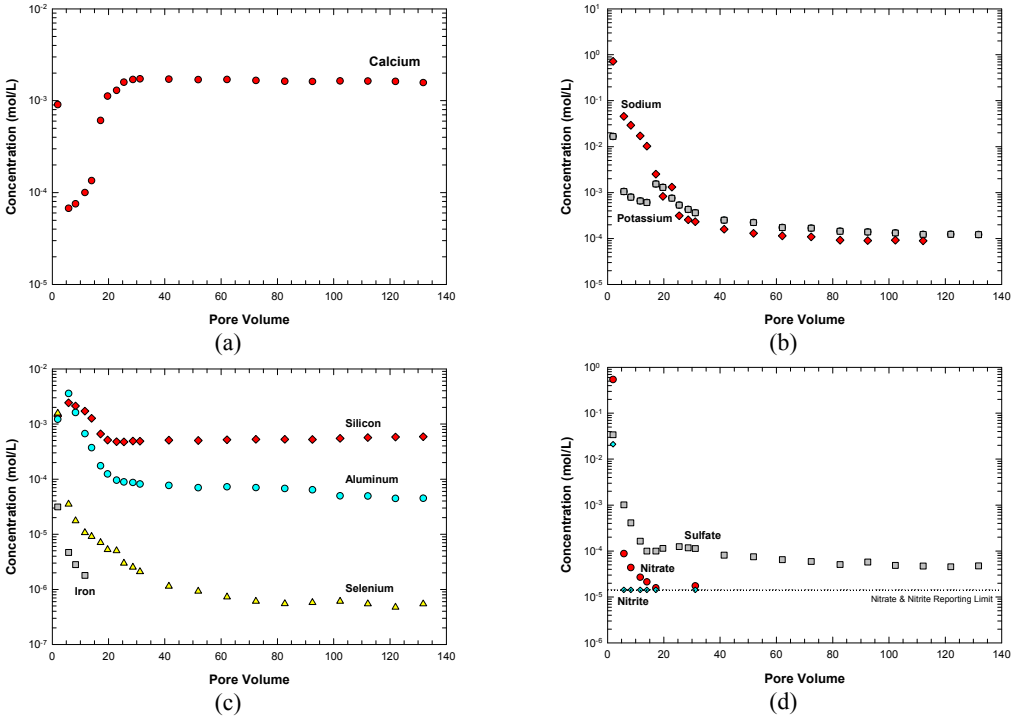

Fig. 2. Measured concentrations of (a) calcium; (b) sodium and potassium; (c) silicon, aluminum, selenium, and iron; and (d) nitrate, nitrite, and sulfate in the effluent solution as a function of number of PVs.

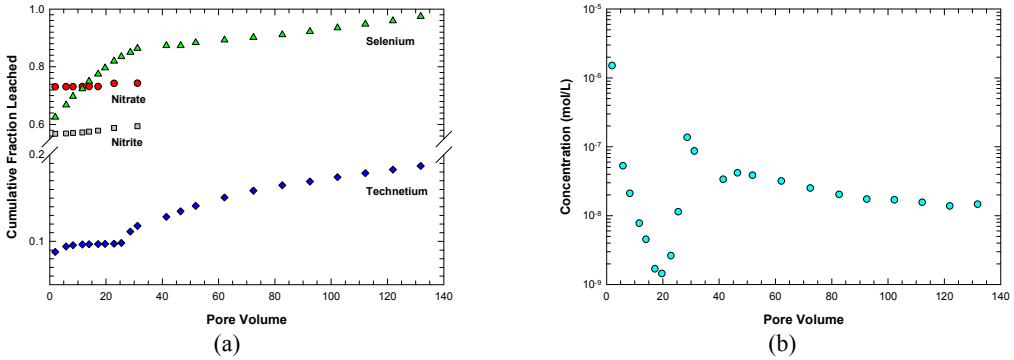

Fig. 3. (a) Calculated cumulative fraction of technetium, selenium, nitrate, and nitrite leached from the grout column and (b) measured technetium concentration in leachant solution as a function of number of PVs

The cumulative fractions of technetium, selenium, nitrate, and nitrite leached at 2 PVs were 0.088, 0.63, 0.73, and 0.57, respectively. The small fraction of technetium released very early in the experiment at high concentration (Figure 3b) likely was leached from the reducing grout that was oxidized during preparation of the crushed material. Nitrate and nitrite leaching essentially were negligible after 20 PVs as their aqueous concentrations were below the reporting limit of the analytical method. In contrast, selenium was continuously released, reaching a cumulative fraction leached of 0.97 at 132 PVs. The selenium data are consistent with those of Gerdes, et al. [14], who stated that slag-bearing saltstone does not retain much of the selenium initially in the grout and that essentially all of the selenium is released during leaching.

Following the initial technetium release, the technetium cumulative fraction leached was relatively constant at ~0.1 up to ~26 PVs. Beyond 26 PVs, the cumulative fraction leached increased with increasing PV and was 0.19 at 132 PVs. Additional data collected from a similar experiment reported in [13] indicated that ~50 percent of the initial technetium remained in the reducing grout, i.e., ~50 percent of the initial technetium was released after 134 PVs. Therefore, the cumulative fraction of Tc leached may have been underestimated in Figure 3a.

An Eh-pH diagram illustrating technetium speciation and the measured effluent Eh and pH are presented in Figure 4(a). The diagram was calculated using Geochemist's Workbench ACT2 Version 7.0 and the thermo.com.v8.r6+.dat thermodynamic database. The circles in Figure 4 are Eh and pH values during the first two PVs of flow, and the diamonds are Eh and pH values at higher

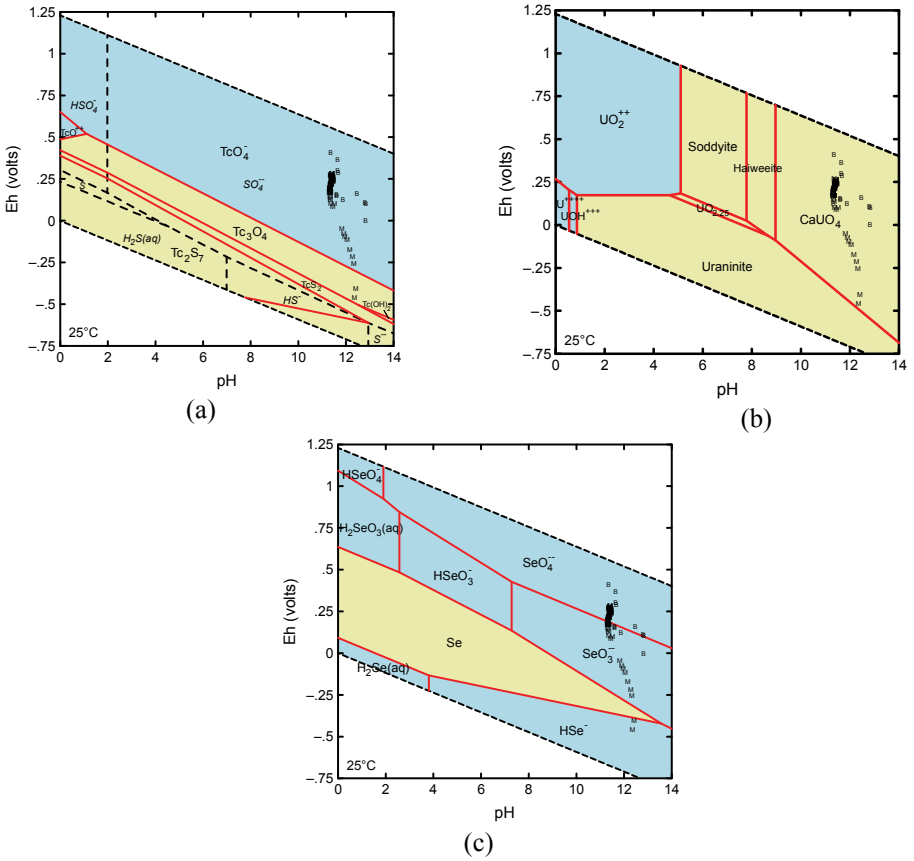

Fig. 4. Eh–pH diagrams calculated using Geochemist's Workbench ACT2 of (a) technetium (TcO_4^- activity = 10^{-8}; SO_4^{2-} activity = 10^{-3}), (b) uranium (UO_2^{2+} activity = 10^{-8}; Ca^{2+} activity = 10^{-3}), and (c) selenium (SeO_3^{2-} activity = 10^{-7}; Ca^{2+} activity = 10^{-3}) speciation. Circles represent Eh–pH values during the first two PVs of flow whereas diamonds represent Eh–pH values at higher PVs. Upper and lower dashed lines bound the water stability field.

PVs. The figure indicates that after two PVs of solution flow, the experimental system chemistry attained Eh conditions (as low as −453 mV at 6.5 PVs) in which technetium solubility is low, constrained by the solubility of the Tc_3O_4 phase.

At 7.2 PVs, the system Eh is significantly higher (–250 mV), which is in the stability field of the pertechnetate ion. This transition was expected to correspond to a significant increase in technetium release. However, data in Figure 3 shows that up to 26 PVs, technetium release was relatively small and constant even though the system Eh has transitioned into the pertechnetate ion stability field. The time lag between Eh increase and technetium release possibly is due to slow oxidation of technetium at depth within the grout particles, which in turn is likely controlled by O_2 diffusion into the particles. Although the effluent Eh reflects oxidized conditions, the groundwater simulant may not have reacted fully with reductants within the interior of the saltstone particles. As stated in a preceding paragraph, additional data reported in [13] indicated that only ~50 percent of the initial technetium was released after 134 PVs and a significant fraction remained unoxidized. The evolution of groundwater chemistry is expected to be a function of a number of variables, including groundwater flow rate through the system. The effect of these variables will be studied in future experiments.

An alternative explanation is that technetium may have remained in the relatively insoluble Tc(IV) oxidation state even though the measured system Eh indicates that Tc(VII) would be thermodynamically favored. Some published studies indicate that certain forms or occurrences of Tc(IV) can be exceedingly resistant to oxidative remobilization [15]. Published studies [16,17] show that TcO_4^- ions can be effectively reduced and coprecipitated by FeS_2, forming a TcS_2-like product, but that reoxidation of the FeS_2 host with aging resulted in technetium forming a TcO_2-like phase, rather than being oxidized back to the TcO_4^- ion.

Figure 4(b) shows an Eh-pH diagram of uranium speciation. The measured effluent solution pH and Eh, also plotted in the figure, lie within the $CaUO_4$ stability field. $CaUO_4$ has low solubility, with a log K_{sp} of −15.74 [18], and quite possibly mitigated uranium release from the grout. In contrast to technetium and uranium, selenium release from the reducing grout was not solubility limited. Figure 4(c) shows an Eh–pH diagram of selenium speciation. The measured Eh–pH after two PVs was in the region where selenium likely was present as an aqueous HSe^- species and its release would not have been solubility limited. Although selenium metal could precipitate as the Eh increased and, thus, inhibit selenium release, selenium metal stability is limited to a narrow range of Eh and its formation may have been too slow to significantly hinder selenium release.

4 Summary and Conclusions

A column experiment was conducted to study technetium, uranium, and selenium release from a reducing grout similar in composition to SRS saltstone. The data show that uranium was retained in the grout most likely as a $CaUO_4$ phase, whereas almost all of the selenium was released during the timeframe of the experiment. Technetium release from the simulated saltstone was relatively constant until 26 PVs, and then afterwards increased significantly with increasing PV. The increase in technetium release was slightly delayed relative to the observed increase in Eh. The system Eh and pH started under conditions in which technetium solubility is low, constrained by Tc_3O_4 solubility, but eventually transitioned into the stability field of the pertechnetate ion. The time lag between increased Eh and increased technetium release possibly was due to slow oxidation of technetium at depth within the grout particles, which in turn was likely controlled by O_2 diffusion into the particles. Alternatively, a low solubility, metastable Tc(IV) phase could have formed that is resistant to oxidative remobilization. In contrast to technetium and uranium, selenium release was not solubility limited and selenium likely was present in the grout pore solution initially as a HSe^- species.

Acknowledgments

This paper was prepared to document work performed by the Center for Nuclear Waste Regulatory Analyses (CNWRA®) for the U.S. Nuclear Regulatory Commission (NRC) Office of Federal and State Materials and Environmental Management Programs, Division of Waste Management and Environmental Protection under Contract No. NRC–02–07–006. This paper is an independent product of the CNWRA and does not necessarily reflect the view or regulatory position of NRC. The NRC staff views expressed herein are preliminary and do not constitute a final judgment or determination.

References

1. B.G. Brodda, Sci. Total Environ. **69**, 319 (1988)
2. A. Aloy, E.N. Kovarskaya, J.R. Harbour, et al., Mat. Res. Soc. Symp. Proc. **985**, 367 (2007)
3. M. Atkins and F.P. Glasser, Waste Management **12**, 105 (1992)
4. W.W. Lukens, J.I. Bucher, D.K. Shuh, and N.M. Edelstein, Environ. Sci. Tech. **39**, 8,064 (2005)
5. Y. Liu, J. Terry, and S. Jurisson, Radiochim. Acta **95**, 717 (2007)
6. G. Baston, M. Brownsword, J. Cross, et al., *The Solubility of Uranium in Cementitious Near-field Chemical Conditions* (Nirex Ltd., United Kingdom, 1990)
7. I. Baur and C.A. Johnson, Environ. Sci. Tech. **37**, 3,442 (2003)
8. S.L. Painter and R.T. Pabalan, *Estimated Longevity of Reducing Environment in Grouted Systems for Radioactive Waste Disposal* (Center for Nuclear Waste Regulatory Analyses, San Antonio, Texas, 2009)
9. M. Denham, *Estimation of Eh and pH Transitions in Pore Fluids During Aging of Saltstone and Disposal Unit Concrete* (Savannah River National Laboratory, Aiken, South Carolina, 2008)
10. D. Kaplan, K. Roberts, J. Coates, et al., *Saltstone and Concrete Interactions With Radionuclides: Sorption (Kd), Desorption, and Reduction Capacity Measurements* (SRR-CWDA-2010-00128, Rev. 1, Savannah River National Laboratory, Aiken, South Carolina, 2008)
11. Savannah River Remediation Closure and Waste Disposal Authority, *Performance Assessment for the Saltstone Disposal Facility at the Savannah River Site* (Savannah River Remediation Closure and Waste Disposal Authority, Aiken, South Carolina, 2009)
12. R.N. Strom and D.S. Kaback, *SRP Baseline Hydrogeologic Investigation: Aquifer Characterization, Groundwater Geochemistry of the Savannah River Site and Vicinity*, (Westinghouse Savannah River Company, Aiken, South Carolina, 1992)
13. R.T. Pabalan, G.W. Alexander, and D.J. Waiting, *Experimental Study of Contaminant Release From Reducing Grout* (Center for Nuclear Waste Regulatory Analyses, San Antonio, Texas, 2012)
14. K.D. Gerdes, J.R. Harbour, J.C. Marra, et al., *The U.S. Department of Energy–Office of Environmental Management's International Program*. Waste Management'07 Conference, February 25–March 1, 2007, Tucson, Arizona
15. J.K. Fredrickson, J.M. Zachara, A.E. Plymale, et al., Geochim. Cosmochim. Acta **73**, 2,299 (2009)
16. M.J. Wharton, B. Atkins, J.M. Charnock, et al., Applied Geochem. **15**, 347 (2000)
17. Y. Liu, J. Terry, and S. Jurisson, Radiochim. Acta **96**, 823 (2008)
18. I. Grenthe, J. Fuger, R. Konings, et al., *Chemical Thermodynamics, Volume 1: Chemical Thermodynamics of Uranium* (North-Holland, Amsterdam, 1992)